Virtual Reality for Prostate Gland Cryosurgery

R. Joan-Arinyo
Divisió d'Informàtica Gràfica
Centre de Recerca en Enginyeria Biomèdica
Universitat Politècnica de Catalunya
Av. Diagonal 647, 8^a, E-08028 Barcelona

Abstract

In this paper we report on the work conducted to develop a computer based system to simulate cryoablation therapy of prostate gland for use in training urologists and surgery planning. The system has been developed on an standard personal computer using standard libraries for graphical output and running the LINUX operating system.

keywords Prostatectomy, surgery simulation, surgery training systems, cryosimulation.

1. Introduction

The prostate is a fibro-muscular gland with a chestnut size located below the bladder of human males. The urethra passes through the prostate longitudinally from the bladder to the verumontanum. Distal to the verumontanum is the sphincter mechanism which is responsible for the urinary continence. Figure 1 illustrates the anatomy of the pubic zone of a human male showing the bladder, prostate and urethra.

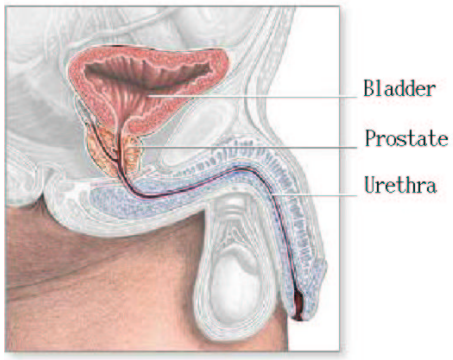

Figura 1: Prostate anatomy.

Prostate cancer is one of the top leading causes of cancer deaths in West World's men, [3, 6]. Traditional treatments for prostate cancer include surgical removal or radiation therapy.

Cryosurgery is a minimally invasive cancer treatment whose origins go back to the 1880s when advanced carcinoma of the breast and uterine cervix were treated with iced saline solutions. [7]. Recently, however, cryosurgery has been accepted as a treatment option in localized carcinoma of the prostate, in part because of new technological advances, [10, 19], in part because it has certain advantages over other procedures such as lower morbidity, minimal blood loss, and a shorter hospital stay. The technique has been described in numerous papers. See for example [2, 9, 12, 14, 15, 16, 18],

Prostate cryosurgery uses liquid nitrogen or supercooled argon to freeze and thus destroy tumors. Liquid nitrogen cools the tumor via a set of cryoprobes which have adjustable flow rates, cooling temperatures, and activation times. See Figure 2. The temperature of the leading front of the iceball that freezes the tissue is -8°C, the temperature needed to kill the tissue has been reported to be between -40° and -50°, [17].

In this paper we report on the work conducted to develop a computer based system to simulate cryoablation therapy of prostate gland for use in training urologists. The system has been developed on an standard personal computer using standard libraries for graphical output and running the LINUX operating system.

The rest of the manuscript is organized as follows. Section 2 presents the thermodynamical model used. Section 3 introduces the geometric model used to represent the constituents of the prostate

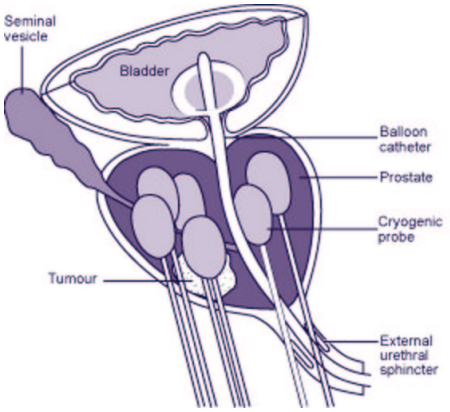

Figura 2: Prostate anatomy and cryosurgical instruments.

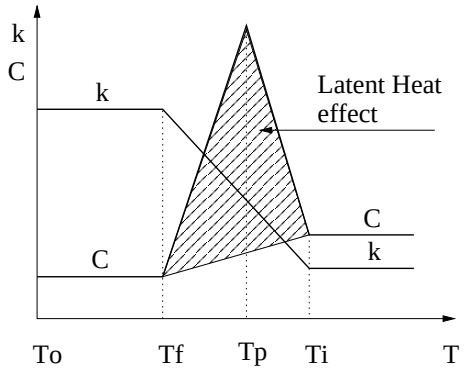

Figura 3: Estimation of heat capacity and thermal conductivity in phase change zone.

gland. Section 4 gives the details of the implementation. Section 5 reports the results yielded by the simulator for several cases. Section 6 offers a short conclusion.

2. Freezing of Living Tissues and Heat Transfer Model

The macroscopic aspects of freezing in living tissues are taken from Comini *et al.* [5]. The heat transfer model used in this work is taken form Rabin *et al.* [14]. We include them here for the sake of completeness.

2.1. Freezing in Living Tissues

In most of the biological substances water is the major component. Thus, when these materials are cooled below 0°C, ice formation occurs, starting at temperature T_i, usually in the vicinity of -1°C, which depends on the molar concentration of the soluble cell components. As the temperature is progressively reduced, more and more water is turned into ice and the latent heat of ice formation adds to the sensible heat involved in cooling both ice and the unfrozen solution. This leads to large variations in heat capacity with respect to temperature, while thermal conductivity also changes considerably, mainly because the thermal conductivity coefficient of ice is almost four times greater than that of water.

For most biological materials the largest part of the freezing process takes place in a temperature interval between -1 and -8°C, while the largest variations of heat capacity occur between -1 and -3°C. Only at temperatures ranging from -20 to -40° and below is there no more measurable change with temperature in the amount of ice present, and the remaining water, if any, can be considered as non-freezable. However, for practical purposes, a lower limit T_f to the phase change interval can be defined on the basis of a ratio of ice to total water content of, say, 90 percent. This choice, in addition to providing an easily applicable criterion, allows one to approximate heat capacity and thermal conductivity curves below T_f by means of constant values. Following Bonacina [1] and Comini [4] we will use a triangle and straight line to interpolate heat capacity and thermal conductivity of biological materials in the phase-change zone. See Figure 3. Different shapes for the interpolating curves have also been tested but improvements obtained, if any, do not justify additional complications, [1].

2.2. Heat Transfer: The Transient

It is generally assumed, see for example Rabin, [14], Jankun *et al.* , [9], Wojtowicz *et al.* , [18], that the heat transfer in those biological tissues characterized by a dense capillary network and low blood perfusion can be modeled by the classical bioheat equation reported by Pennes, [11],

$$C\frac{\delta T}{\delta t} = \bigtriangledown \cdot (k \bigtriangledown T) + \dot{w}_b C_b (T_b - T) + \dot{q}_{met} \quad (1)$$

where C, T and k are, respectively, the volume specific heat, temperature and the thermal conductivity of the prostatic tissue, T_b is the blood temperature, $\dot{w}_b C_b$ is the blood perfusion rate, and $\dot{q}_{met}$ is the volumetric heat source.

Although the general validity of this model is questionable, Rabin *et al.* showed in [13] and [14] that the model can be used for engineering calculations and especially to simulate the bahviour of cryosurgical probes. If i, j, k stand for the coordinates of a numerical grid points in a three-dimensional space, Equation 1 can be discretized in finite differences as follows

$$\mathrm{C}_{i,j,k}\frac{T^{t+1}_{i,j,k} - T^{t}_{i,j,k}}{\Delta t} = \frac{1}{\Delta V_{i,j,k}} \sum_{l,m,n} \frac{T^{t}_{l,m,n} - T^{t}_{i,j,k}}{R_{l,m,n-i,j,k}}$$

$$+ (\dot{w}_b C_b)_{i,j,k} (T_b - T^{t+1}_{i,j,k}) + (\dot{q}_{met})_{i,j,k} \quad (2)$$

where l, m and n are spatial indices for all the grid points in the neighbourhood of node i, j, k. According to Rabin, [14], the heat source term of blood perfusion in Equation 2 is specified at time level $t+1$, although the other terms on the right-hand side of the equation are written at time level t. This presentation would result in an increase of the stability of the numerical integration method.

If $R_{l,m,n-i,j,k}$ is the thermal resistance to heat transfer by conduction from grid point i, j, k to its neighbouring grid points l, m, n, [14], and we define

$$K = \frac{\Delta t}{\Delta V_{i,j,k} (C_{i,j,k} + (\dot{w}_b C_b)_{i,j,k} \Delta t)}$$

rearranging Equation 2 yields

$$\mathrm{T}^{t+1}_{i,j,k} = K \sum_{l,m,n} \frac{T^{t}_{l,m,n} - T^{t}_{i,j,k}}{R_{l,m,n-i,j,k}}$$

$$+ \frac{\Delta t [(\dot{w}_b C_b)_{i,j,k} T_b + (\dot{q}_{met})_{i,j,k}] + C_{i,j,k} T^{t}_{i,j,k}}{C_{i,j,k} + (\dot{q}_{met} C_b)_{i,j,k} \Delta t} \quad (3)$$

where the thermophysical properties, blood perfusion and metabolic heat generation are temperature dependent and thus have to be evaluated at each time level for each grid point.

According to Rabin *et al.* [14], using standard stability techniques, it can be shown that the stability criterion for the case of no blood perfusion is

$$\Delta t = \left[\frac{(\Delta VC)_{i,j,k}}{\sum_{l,m,n} (1/R_{l,m,n-i,j,k})} \right]_{min} \quad (4)$$

This stability criterion is necessary but not sufficient for calculating the maximal time step. An additional criterion is derived from energy conservation considerations. Time steps should be selected such that the temperature at each grid point of the phase transition region would change over a number of successive time steps. This will ensure that the latent heat effect is included in its entirety by the function representing the effective specific heat.

The stability criterion given by Equation 4 requires relatively short time intervals, which seems to be the major drawback of the numerical scheme proposed. Therefore, it seems that any unconditionally stable numerical scheme would be preferable for the solution of the freezing problem, as there are no limitations on the length of time intervals. Regardless of the chosen numerical technique, the nature of the freezing process during cryosurgery, i.e., dramatic changes in thermophysical properties and steep temperature gradients, will demand a relatively fine numerical grid distribution. In turn, this will demand a relatively short time interval from energy conservation considerations, as mentioned above. For example, Rabin *et al.* show in [13] that four to five numerical grid points are required within the phase transition temperature range, at any given time. Therefore, the unconditionally stable numerical techniques do not automatically guarantee shorter time intervals for the particular problem of freezing of biological tissues.

2.3. Heat Transfer: The Steady State

The steady state can be solved by running the transient solution, that is, integrating Equation 2 until a steady state is reached. However, due to the stability criterion associated with the numerical scheme, which leads to very small time intervals, the transient approach as a means of generating a steady state solution is very expensive.

At steady state, the left side term of Equation 2 becomes zero, which leads to the following numerical scheme

$$0 = \sum_{l,m,n} \frac{T_{l,m,n} - T_{i,j,k}}{R_{l,m,n-i,j,k}}$$

$$+ (\dot{w}_b C_b)_{i,j,k} (T_b + T_{i,j,k}) (\dot{q}_{met})_{i,j,k} \quad (5)$$

The metabolic heat generation term is included here only for consistency in presentation with the bioheat equation.

Equation 5 is solved simultaneously for all grid points using an iterative predictor-corrector scheme.

3. Geometric Model of the Prostate Gland

A voxel-based volumetric object is a regular or irregular 3D array of data, with each element representing a sampled point (measured o calculated) in the volume. For cryosurgery simulation, this representation has a number of advantages over the use of polygons or solid geometric primitives. First, because the data organization is the same as the acquired data, a voxel-based representation is natural for the 3D digital images produced by medical scanning technologies such as MRI or Computed Tomography (CT). Second, since no surface extraction or other data reformatting is required, errors introduced by fitting surfaces or geometric primitives to the scanned images can be avoided. Finally, volumetric objects can incorporate detailed information about the internal anatomical or physiological structure of organs and tissues. This information is particularly important for realistic modeling and visualization of complex tissue volumes.

We created a 3D volume model of the prostate gland based on discretizing by hand a plastic made physical model of natural size. The model includes the capsule, prostatic tissue, the urethra, and the blood vessels.

The anatomical objects are represented using a generalized voxel model, [8], in a 3D rectilinear grid with an spatial resolution of 0.1 mm. The Z axis along the urethra has 194 voxels while X and Y axis on a plane normal to the Z axis, have 256 and 202 voxels, respectively. Each voxel is associated with a set of attributes such as its membership to anatomical regions or color and.

Figure 4 depicts the textured prostate model. The bladder depression can be seen at the top of the prostate. The urethra is at the bottom. Figure 5 depicts the prostate as a transparent model showing the urethra.

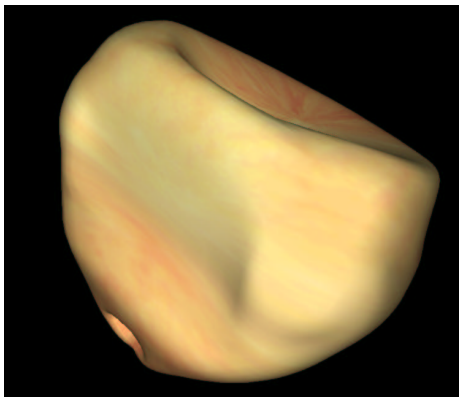

Figura 4: Prostate textured model.

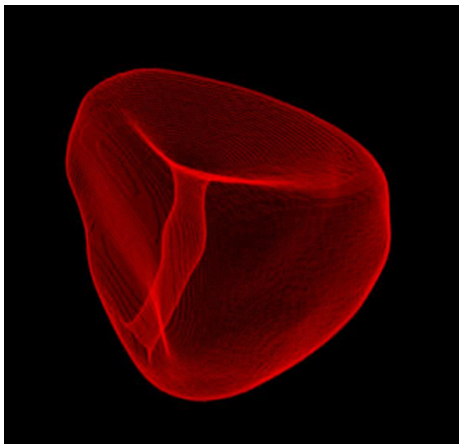

Figura 5: Transparent view of the prostate.

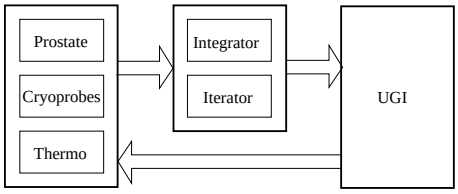

Figura 6: System architecture.

4. Implementation

We have implemented a computer program to model cryosurgery mathematically. The program solves the heat transfer problem by integrating, in a very low spatial resolution, the partial differential equation that models the physical phenomenon, as described in Section 2.

The program has been developed on a personal computer with a Pentium III at 600 MHz, 386MB in central core running under GNU/Linux, and a Nvidia Geforce 4400 with 256 MB. The programming language used was **C** and the graphics library used for rendering was OpenGL from Nvidia.

The system has three different main components: The user graphic interface, Figure 6 right, the solver, Figure 6 middle, and the model, Figure 6 left. The user interface, implemented using the Gnome ToolKit (GTK+) library, provides tools to select the number of cryoprobes to be included as well as the placement for each of them. Other variables the user can fix are the length of the cooling cryoprobe tip, cooling temperature, coolant flow rate and the total time of evolution. As output tools, the user interface allows standard operations like zooming in and out, selecting cross sections and selecting specific voxels from the graphic output to show the exact temperature at a given point.

The solver, the unit that actually carries out the computations, includes two units: the integrator, which solves the transient problem by integrating the differential equation , and the iterator, which solves the system of equations for the steady state.

The model includes three different units. The Prostate unit models the prostatic geometry as explained in Section 3. The Cryoprobes unit models the cryoprobes geometry. The Thermo unit collects all the data concerning the thermodynamic properties of the materials in the system.

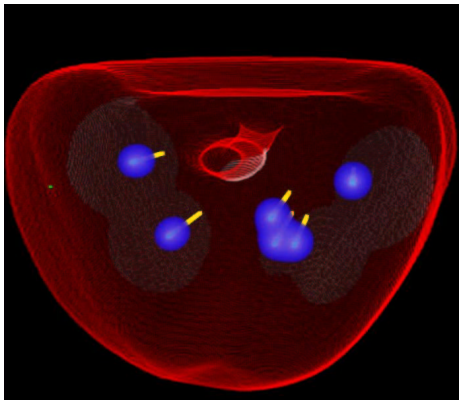

Figura 7: Prostate with cryoprobes. Frontal view.

5. Results

To assess the applicability of the software implemented, we have fed the program with a number of cases that span different aspects of the simulated thermodynamic system. We show the results yielded by the program for cryoprobe coolant tips of 5mm and coolant temperature of -160°C. Temperature in the iceballs is represented using a scale of colors varying linearly from dark blue for 0°C to white for -160°C.

Figures 7, 8 and 9 show, respectively, frontal, side and top views, of the prostate with six cryoprobes and the iceballs formed. The cryoprobes are placed at a distance from each other such that the iceballs formed by three of them do not overlap while the iceballs formed by the remaining three cryoprobes overlap.

Figure 10 depicts a cross section showing the overlapping iceballs. Figure 11 shows a zoom in of the three overlapping iceballs where the resulting lethal area can be seen clearly.

A temperature difference of less than 10^{-3} °C was used as a threshold for convergence in our studies. When integrating the differential equation in the transient study, reaching the steady state required more than 10^6 iterations along the transient. This means a computation time larger than six hours. In the steady state computation, typically, 50

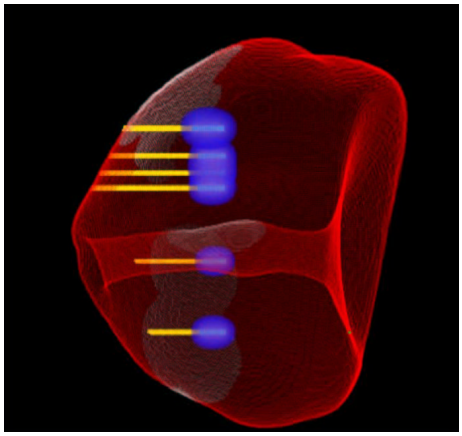

Figura 8: Prostate with cryoprobes. Side view.

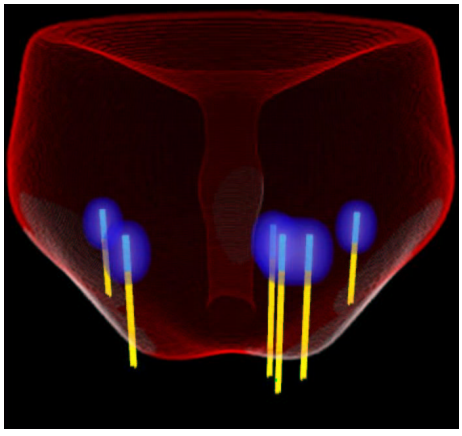

Figura 9: Prostate with cryoprobes. Top view.

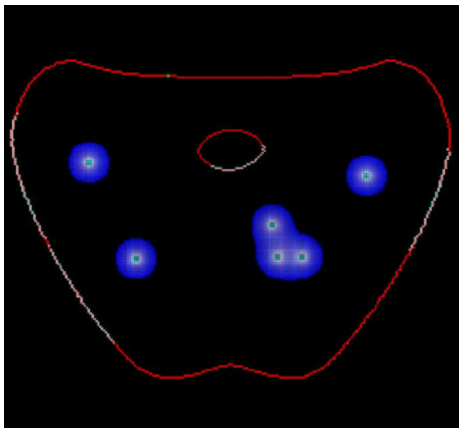

Figura 10: Prostate with cryoprobes. Cross section.

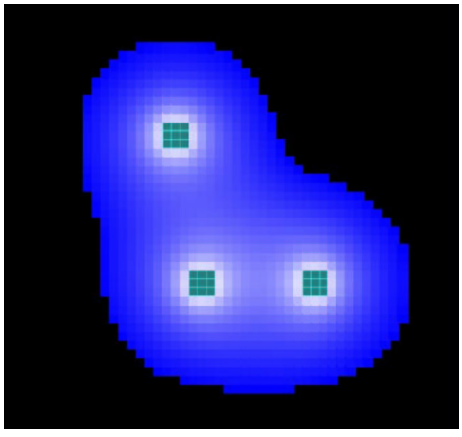

Figura 11: Three overlapping cryoprobes.

to 70 prediction-correction cycles were required to reach a steady state solution. This means a computation time of about 30 minutes.

6. Conclusions

We described the implementation of a software system to model cryoablation therapy for prostate cancer. The system solves the heat transfer problem by integrating in a very low spatial resolution, the partial differential equation that models the physical phenomenon.

The system provides a platform for accurate cryosurgery planning and training of novel surgeons. However, computation time needed to integrate the differential equation in the transient study is too long and techniques to shortening it must be devised.

Acknowledgements

This research has been partially funded by the Centre de Referència en Enginyeria Biomèdica de Catalunya (CREBEC) and by the Red de Grupos del Instituto Carlos III, IM^3: Imagen Molecular y MultiModalidad. The author thanks Mr Pau Baiget for his efforts in implementing the software.

Referencias

[1] C. Bonacina and *et al*. On the estimation of thermophysical properties in nonlinear heat conduction problems. *International Journal of Heat Mass Transfer*, 17:861–867, 1974.

[2] H.M. Budman, J. Dayan, and A. Shitzer. Crontolled freezing of nonideal solutions with applications to cryosurgical processess. *Journal of Biomechanical Engineering*, 113:430–437, 1991.

[3] L.X. Clegg, F.P. Li, B.F. Hankey, K. Chu, and B.K. Edwards. Cancer survival among US whites and minorities: a SEER (Surveillance, Epidemiology and End Results) programm population-based study. *Archives of Intenational Medicine*, 162:1985–1993, 2002.

[4] G. Comini, C. Bonacina, and S. Barina. Thermal properties of foodstuffs. *Annexe 1974-3 au Bulletin IIF*, 1974.

[5] G. Comini and S Del Giudice. Thermal aspects of cryosurgery. *Journal of Heat Transfer*, 98(4):543–549, November 1976.

[6] E. Giovannucci, M. Leitzmann, D. Spiegelman, E.B. Rimm, G.A. Colditz, and M.J. Stampfer. A prospective study of physical activity and prostate cancer in male health professionals. *Cancer Research*, 58:5117–5122, 1998.

[7] N.E. Hoffmann and J.C. Bischof. The cryobiology of cryosurgical injury. *Urology*, 60:40–49, 2002.

[8] K.H. Höne, M. bomans, A. Pommert, M. Riemer, C. Schiers, U. Tiede, and G. Wiebecke. 3D visualization of tomographic volume data using the generalized voxel-model. *Visual Computer*, 6(1):28–36, 1990.

[9] M. Jankun, T.J. Kelly, A. Zaim, K. Young, R.W. Keck, S. Selman, and J. Jankun. Computer model for cryosurgery of the prostate. *Computer Aided Surgery*, 4:193–199, 1999.

[10] G.M. Onik, B. Watson, and R.J. Ablin. Percutaneous prostate cryoablation. St. Louis, MO: Quality Medical, 1995.

[11] H.H. Pennes. Analysis of tissue and arterial blood temperature in resting human forearm. *Journal of Applied Physiology*, 1(2):93–122, August 1948.

[12] J. Poledna and W. Berger. A mathematical model of tenperature distribution in frozen tissue. *Gen. Physiol. Biophysiscs*, 15:3–155, 1986.

[13] Y. Rabin, R. Coleman, R. Mohordohovich, D. Ber, and A. Shitzer. A new cryosurgical device for controlled freezing. Part II. in vivo experiments on rabbits' hindlimbs. *Cryobiology*, 33:93–105, 1996.

[14] Y. Rabin and A. Shitzer. Numerical solution of the multidimensional freezing problem during

cryosurgery. *ASME Journal of Biomechanical Engineering*, 120(32):193–199, February 1998.

[15] J.C. Rewcastle, G.A. Sandison, L.J. Hahn, J.C. Saliken, J.G. McKinnon, and B.J. Donnelly. A model for the time dependent thermal distribution within an iceball surrounding a cryoprobe. *Phys. Medical Biology*, 43:3519–3534, 1998.

[16] M.A. Richmond, C.A. Murphy, B. Pouzet, P. Schmid, J.N. Rawlins, and J. Feldon. A computer controlled analysis of freezing behaviour. *Journal of Neuroscience Methods*, 86:91–99, 1998.

[17] K. Tatsutani, B. Rubenski, G. Onij, and R. Dahiya. Effect of thermal variables on frozen human primary prostatic adenocarcinoma cells. *Urology*, 48:441–447, 1996.

[18] A. Wojtowicz, S. Selman, and J. Jankun. Computer simulation of prostate cryoablation-fast and accurate approximation of exact solution. *Computer Aided Surgery*, 8:91–98, 2003.

[19] W.S. Wong, D.O. Chinn, M. Chinn, J. Chinn, and W.L. Tom. Cryosurgey as a treatment of prostate carcinoma. *Cancer*, 79:963–974, 1997.